Biochemical and Biophysical Research Communications 443 (2014) 313–320

Contents lists available at ScienceDirect

Biochemical and Biophysical Research Communications

journal homepage: www.elsevier.com/locate/ybbrc

Transgenic mice expressing mutant Pinin exhibit muscular dystrophy, nebulin deficiency and elevated expression of slow-type muscle fiber genes

Hsu-Pin Wu [a,1], Shu-Yuan Hsu [a,1], Wen-Ai Wu [b], Ji-Wei Hu [b], Pin Ouyang [a,b,c,*]

[a] Department of Anatomy, Chang Gung University Medical College, Taiwan
[b] Transgenic Mouse Core Laboratory, Chang Gung University, Taiwan
[c] Molecular Medicine Research Center, Chang Gung University, Taiwan

ARTICLE INFO

Article history:
Received 18 November 2013
Available online 2 December 2013

Keywords:
Pinin
Muscular dystrophy
Nebulin
Slow type fiber gene

ABSTRACT

Pinin (Pnn) is a nuclear speckle-associated SR-like protein. The N-terminal region of the Pnn protein sequence is highly conserved from mammals to insects, but the C-terminal RS domain-containing region is absent in lower species. The N-terminal coiled-coil domain (CCD) is, therefore, of interest not only from a functional point of view, but also from an evolutionarily standpoint. To explore the biological role of the Pnn CCD in a physiological context, we generated transgenic mice overexpressing Pnn mutant in skeletal muscle. We found that overexpression of the CCD reduces endogenous Pnn expression in cultured cell lines as well as in transgenic skeletal muscle fibers. Pnn mutant mice exhibited reduced body mass and impaired muscle function during development. Mutant skeletal muscles show dystrophic histological features with muscle fibers heavily loaded with centrally located myonuclei. Expression profiling and pathway analysis identified over-representation of genes in gene categories associated with muscle contraction, specifically those related to slow type fiber. In addition nebulin (NEB) expression level is repressed in Pnn mutant skeletal muscle. We conclude that Pnn downregulation in skeletal muscle causes a muscular dystrophic phenotype associated with NEB deficiency and the CCD domain is incapable of replacing full length Pnn in terms of functional capacity.

1. Introduction

Pinin (Pnn) was first characterized as a desmosome-associated protein [1,2]. Subsequently it was found co-localized with splicing factors within the nuclear speckles [3]. Using proteomic analysis, a total of 146 known proteins as well as 32 uncharacterized proteins of nuclear speckles were identified [4]. Given the fact that Pnn was identified in the speckle fraction and the ability of Pnn to interact with splicing proteins SRp75, SRm300 and SRp130 via its C-terminal RS domain [5], and with RNPS1 via its N-terminal coiled-coil domain [6], it is plausible that Pnn participates in mRNA splicing regulation. In addition, proteomic analysis of the spliceosome identified Pnn not only in catalytically active complex C [7], but also in the exon junction complex [8], suggesting that Pnn may also take part in mRNA biogenesis via regulation of splicing as well as nuclear export of mRNA.

Skeletal muscle formation is a multistep process from stem cells to myotubes, which encompasses the transition of many muscle-specific splicing factors and alternative splicing of large proteins during myogenesis and development. Deep-sequencing analysis of different human tissue shows that skeletal muscle is one of the tissues with highest number of differentially expressed alternative exons [9]. A prominent example of a shift in alternative splicing in development is cardiac troponin T (cTNT), in which loss of exon 5 occurs from embryo to adult [10]. A number of regulatory RNA binding proteins, including members of the CELF family (CUGBP and ETR3 like), MBNL, hnRNP H and PTB have been shown to regulate muscle-specific alternative splicing events [11]. It is expected that identification of novel muscle-specific transcription regulators will shed light on the underlying mechanism responsible for not only skeletal muscle biogenesis but also the molecular etiology of muscular dystrophy.

The N-terminal region of Pnn is found highly conserved from mammals to *Caenorhabditis elegans*, but the C-terminal RS domain-containing region is absent in lower species. The function and evolutionary origin of N-terminal coiled-coil domain (CCD) is, therefore, of interest. To explore the biological role of the Pnn CCD

* Corresponding author. Address: 259 Wen-Hwa 1st Road, Quei-San, Taoyuan 333, Taiwan.
E-mail address: ouyang@mail.cgu.edu.tw (P. Ouyang).
[1] These authors contributed equally to this work.

0006-291X/$ - see front matter © 2013 Elsevier Inc. All rights reserved.
http://dx.doi.org/10.1016/j.bbrc.2013.11.108

in a physiological context and to find out whether a Pnn mutant without the C-terminal region could replace endogenous Pnn, in this study we generated transgenic mice overexpressing mouse *Pnn* mutant (*Pnn*1-303 sequence based on Drosophila full length *Pnn*, which exclusively contains the CCD) under the control of human skeletal actin (HAS) promoter. The results provide insights into the mechanism underlying Pnn expression regulation and suggest a role for Pnn in skeletal muscle development.

2. Materials and methods

2.1. Cell culture and transfection

The HeLa, U2OS, L6 and C2C12 were cultured in Dulbecco's modified Eagle's medium (DMEM; Invitrogen Gibco., Carlsbad, CA) supplemented with 10% fetal bovine serum plus 1% penicillin–streptomycin–glutamine, and cultured at 37 °C in a humidified chamber with 5% CO_2. The transfection was performed using Lipofectamine 2000 (Invitrogen Gibco) according to the manufacturer's instructions.

2.2. Immunofluorescent microscopy

The cells were transfected with expression vectors encoding myc-tagged pnn1-303. Cultured cells or cryosections (8 μm) from mouse skeletal muscles were incubated with mixed primary antibodies and processed for immunostaining as described previously [12]. Primary antibodies used were mouse anti-myc monoclonal antibody (clone 9E10.2) or chicken anti-myc polyclonal antibody (1:500, Bethyl Laboratories, Montgomery, TX) and rabbit anti-Pnn polyclonal antibody (P3a, 1:500).

2.3. Western blot

Proteins were isolated from the various cell lines 2 days post-transfection. Cells were lysed in 2× sample buffer (5% SDS, 0.25 M Tris pH 6.8, 5% β-Mercaptoethanol, 0.01% Bromophenol Blue) and heated to 95 °C for 10 min. Equal amount of samples were separated by SDS–PAGE and immunoblotting was performed as described previously [12]. Primary antibodies used include mouse anti-Pnn, mouse anti-myc and mouse anti-β-actin (1:3000, Sigma, St. Louis, MO). The peroxidase-labeled blots were developed using an ECL kit (Amersham Pharmacia Biotech, Piscataway, N.J.).

2.4. Transgenic mice

To generate Pnn CCD mutant under the control of HSA promoter, human Pnn open reading frames (nucleotides 1-303) were cut by EcoR1 and XhoI from hPnn1-303/pcDNA3.1 and ligated to pCMVtag3B. Subsequently myc-hpnn1-303 fragments were generated by using NotI and Bsp120I and cloned to pre-digested HSA-VP1 vector to form HSA-myc-hPnn1-303 transgene vector. The transgene vectors were purified for microinjection into fertilized eggs recovered from super-ovulated FVB female mice. HSA-myc-hPnn1-303 transgenic vector contains HSA promoter and VP1 enhancer (a SV40 intron sequence), which can direct expression of Pnn1-303 specifically in skeletal muscle. Mice were maintained according to the guidelines of the Association for Assessment and Accreditation of Laboratory Animal Care. Animal experiments were approved by the Chang Gung University Institutional Animal Care and Use Committee.

2.5. RNA isolation and microarray analysis

The muscle tissue of tibialis anterior (TA) was isolated from 3-month-old mice. Tissue (50–100 mg) was put into a tube containing 1 ml Trizol, and homogenized with a tissue homogenizer (Precellys 24, Stretton Scientific, UK). Samples were centrifuged to remove the debris and polysaccharides and RNA was extracted according to the instruction manual (MDBio, Taipei, Taiwan). The RNA pellet was air-dried and resuspended in RNase free ddH_2O.

The RNA sample expression level diagnosis was sent to Phalanx Biotech Group (Taiwan), and gene expression chip performed with MOA v2.1 mouse OneArray. The differential expression gene lists were outputted by using Gene Ontology biological process analysis and Gene Set Enrichment analysis of the canonical pathway database.

2.6. Semi-quantitative RT-PCR

The cDNAs were synthesized from 2 μg of TA muscle total RNA using oligo$(dT)_{22}$ and MMLV reverse transcriptase (Epicenter, Madison, WI). PCR were performed using cDNA (100 ng), dNTP (2.5 mM), 10× reaction buffer, the indicated primer sets (10 μM; Supplementary Table 1) and Tag polymerase. PCR program was 28–30 cycles each at 95 °C for 3 min, 55 °C for 45 s, and 72 °C for 90 s.

2.7. Histochemical staining

Tissue cryosections were fixed with 3.7% formaldehyde followed by treatment with 0.5% Triton X-100. Sections were stained with hematoxylin and eosin, dehydrated by ethanol, cleared with xylene and then mounted (Entellan new, Millipore, Billerica, MA) and examined with a light microscope.

Connective tissue was stained using a Masson trichrome stain kit (Sigma, St. Louis, MO). The slides were briefly washed out O.C.T by water, allowed to mordant in Bouin's solution overnight. Samples were stained in Biebrich Scarlet-Acid Fuchsin solution and rinsed in deionized water. Slides were placed in a working phosphotungstic/phosphomolybdic acid solution, followed by aniline blue solution and acetic acid (1%). Finally, slides were rinsed with deionized water, dehydrated with alcohol, cleared in xylene and mounted.

3. Results

3.1. Pnn CCD mutant (Pnn1-303) showed reduced endogenous Pnn expression in various cell lines

Our previous study showed that Pnn is well conserved across mammalian species [2]. However, detailed analysis of the database indicated that there is a great divergence in protein coding regions between vertebrate and non-vertebrate Pnn. Only the coiled-coil domains (CCD, including C1, C2 and C3) is highly conserved from mammals to insects (Fig. 1A), suggesting that it is functionally important. This CCD domain, when overexpressed, could inhibit reporter minigene pre-mRNA splicing and partly block bulk mRNA export [6]. Therefore, we speculated that the CCD of Pnn can function as a dominant negative mutant regulating Pnn expression and function.

To investigate whether the Pnn CCD domain can modulate endogenous Pnn expression and function, based on the Drosophila full length Pnn, we generated a Pnn1-303 construct, which contained a myc-tagged mutant Pnn encoding mouse CCD domain, as a tool to study its impact on Pnn expression in various cell lines. Pnn1-303 exhibited a nuclear distribution with a speckle-like pattern, like that of endogenous Pnn (Fig. 1B(a, d, g, j)). Surprisingly, a

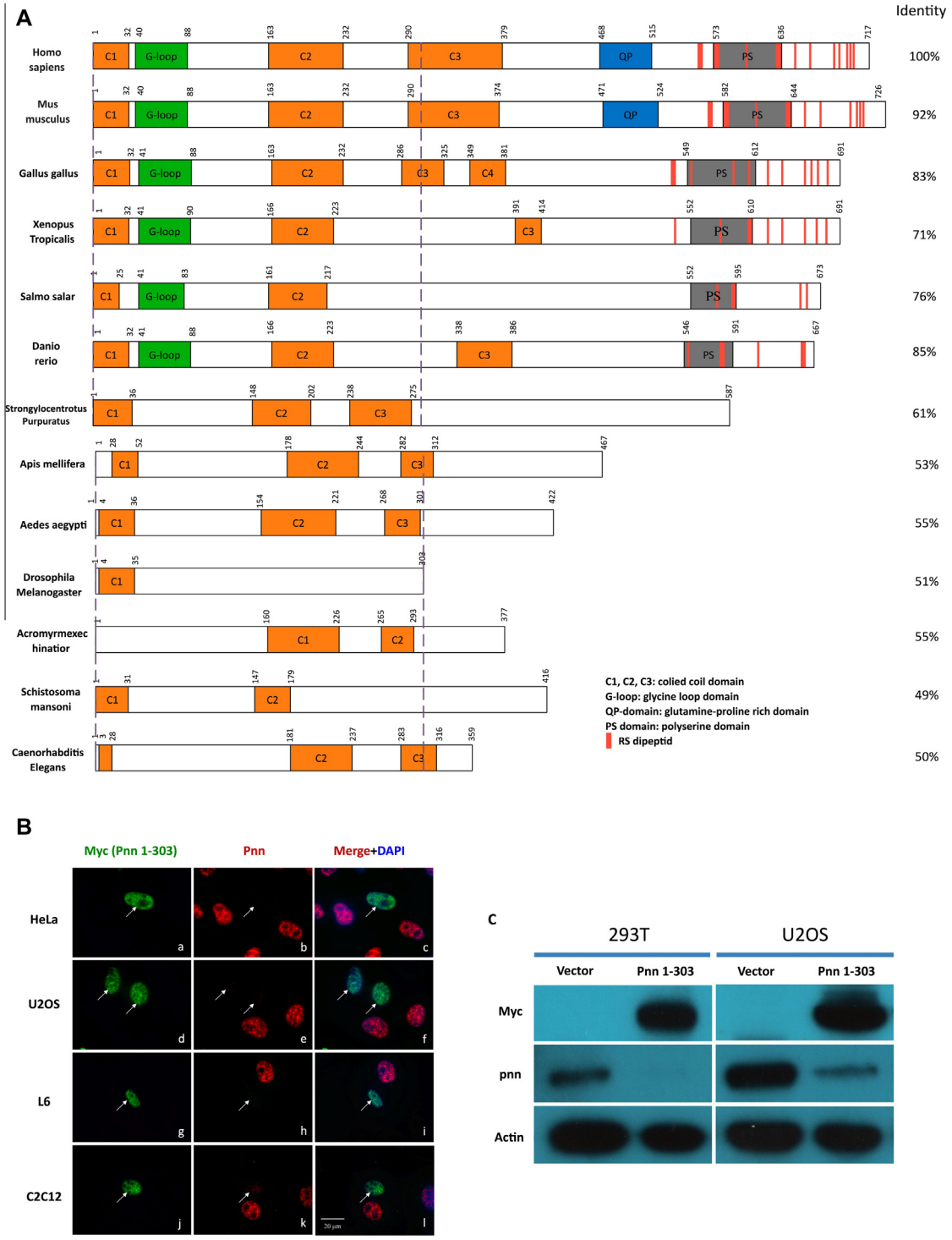

Fig. 1. Expression of Pnn CCD (1-303) mutant reduces endogenous Pnn expression. (A) Schematic of the Pnn structural domain in various animal species. The dashed line indicates the Pnn region spanning amino acids 1-303. (B) Immunofluorescent staining of endogenous Pnn in cell lines transfected with Pnn1-303. Endogenous Pnn expression was downregulated in Pnn1-303 transfected cells (arrows). (C) Western blots demonstrating reduced protein levels of endogenous Pnn by overexpression Pnn mutant in 293T and U2OS cell lines.

dramatic downregulation of endogenous Pnn (Fig. 1B arrows in b, e, h, k) was observed by immunofluorescent staining in various Pnn mutant-transfected human and mouse cell lines. Western blotting confirmed the effect of overexpression of Pnn mutant on reducing endogenous Pnn expression in cultured cell lines (Fig. 1C).

Though repressing endogenous Pnn expression, Pnn CDD mutant overexpression did not reduce the expression of other splicing factors such as SRSF1, SRSF2, RNPS1, or general SR protein nor did it disperse U1A (Supplementary Fig. 1) in nuclear speckles. Taken together these results suggest that the Pnn mutant is efficient at reducing endogenous Pnn expression level, but, unlike Pnn knockdown with RNAi [12], it does not have an effect on the general structural organization of the nuclear speckle domain and protein interaction of common splicing factors.

3.2. Generation of Pnn CCD mutant transgenic (Tg) mice

As endogenous Pnn expression could be modulated by Pnn mutant, we sought to determine whether endogenous Pnn can be replaced physiologically by Pnn mutant. We generated Tg mice overexpressing Pnn CDD mutant in skeletal muscle under the control of HSA promoter. We chose skeletal muscle as our target tissue because previous data showed that negative regulation of Pnn expression impaired striated muscle development in hearts of mouse and zebrafish [13,14] and caused reduced body size in zebrafish. Pnn mutant Tg mice overexpressing Pnn CCD (Fig. 2A) were initially selected following genotyping with genomic PCR

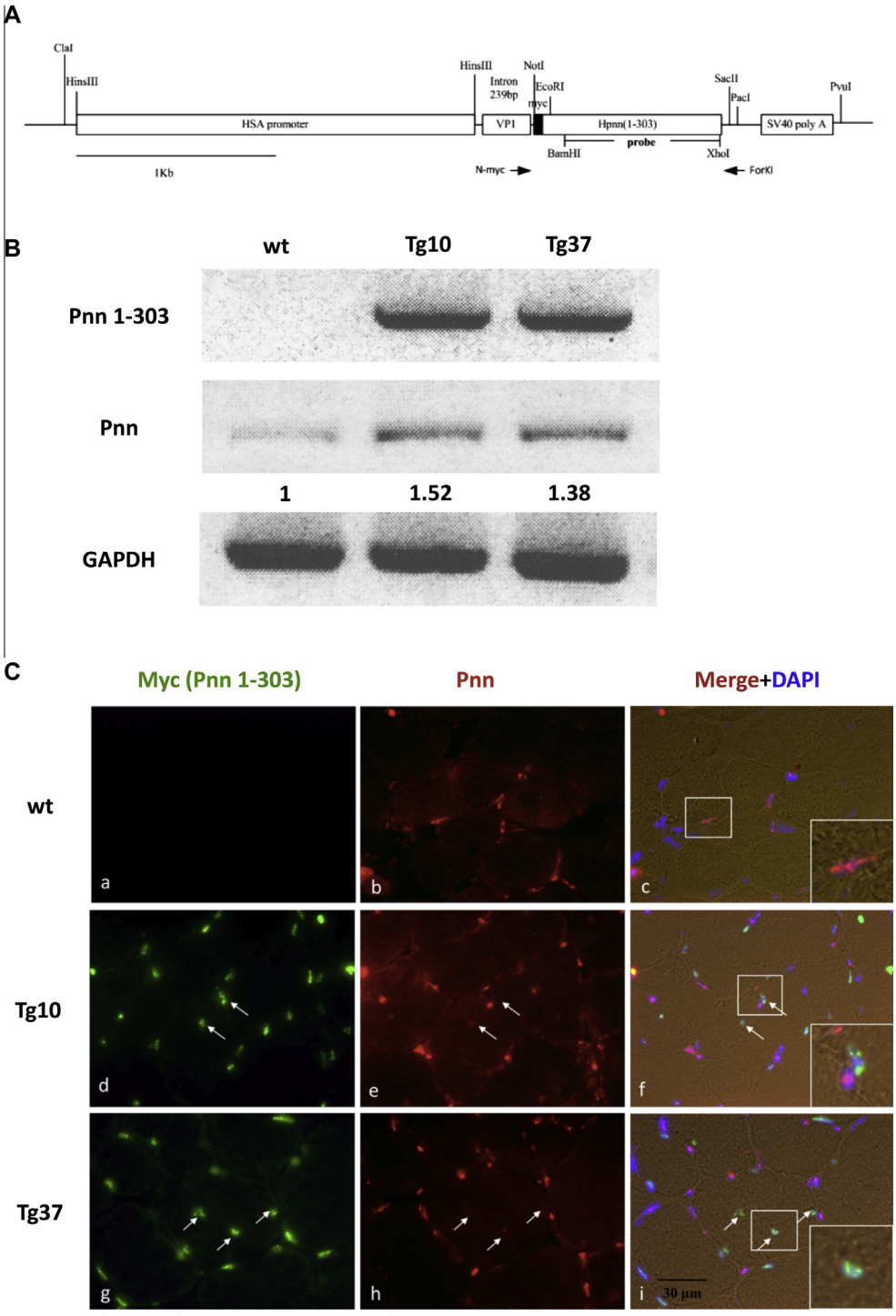

Fig. 2. Reduction of endogenous Pnn expression in Pnn mutant Tg skeletal muscle. (A) Schematic of the structure of the transgene vector. A cDNA encoding Pnn1-303 was placed under the control of HAS promoter with an intron, VP1, between the coding sequence and the promoter. The probe used for Southern blot is shown. Primer set for PCR is denoted with a pair of arrows. (B) RT-PCR demonstrating Pnn CCD mutant signal expression in Tg skeletal muscle. Note that the endogenous Pnn signal was elevated in Tg samples. GAPDH was used as a loading control. (C) Immunofluorescent micrographs of cryo-cross-sections of TA muscle from wild type (a–c), Tg10 (d–f) and Tg37 (g–i) transgenic mice. Pnn1-303 expression reduced endogenous Pnn expression in myonuclei of two different transgenic mice (Tg10 and Tg 37, arrows in e, f and h, i). Muscle cells expressing Pnn1-303 (arrows in d and g) can be identified by myc antibody decorated by FITC fluorescence. Insets show enlargements of the boxed areas in the indicated myofiber.

(Supplementary Fig. 2A) and validated by Southern blot (Supplementary Fig. 2B). We then selected offspring from both founders 10 and 37 for analysis in the subsequent experiments.

As the first step of Tg mouse characterization, we performed RT-PCR to examine whether Pnn1-303 signals can be detected in Tg skeletal muscles. Total RNA was extracted from muscles of wild type (wt), Tg10 and Tg37 mice at 3 months of age. The Pnn mutant signals were detected only in Tg mice but not in wt mice, and the expression levels of endogenous Pnn was elevated to some degree in Tg mice compared to wt mice (Fig. 2B). These data, especially the latter, correlate not only with that presented by microarray profiling of Pnn levels in Tg muscle (1.14-fold increase in log 2 value) but also with our previous report [6], in which we found transfection of the CCD domain can block bulk polyA$^+$-containing RNA nuclear export in a cell line model, leading to mRNA accumulation within the nucleus. Upon immunofluorescent staining of the TA muscle cryosection, Pnn mutant could be identified within nuclei of muscle fibers in Tg10 (Fig. 2C; arrows in d) and Tg37 (Fig. 2C; arrows in g) mice, while endogenous Pnn (Fig. 2C; arrows in e, h) in Tg muscles, but not in wt muscles, clearly showed reduced expression level (compare insets in Fig. 2C(f, i, a–c)). Consistent with decreased endogenous Pnn expression in cell lines as described above (Fig. 1C), Tg muscles express less Pnn as a result of overexpressing mutant Pnn in vivo.

3.3. Overexpression of Pnn mutant leads to a muscle wasting phenotype in transgenic mice

We next analyzed whether Pnn mutant with downregulation of endogenous Pnn expression resulted in impaired skeletal muscle development in Tg mice. First, we monitored comparative body mass between wt and Tg mice from 4 to 12 weeks of age. Tg mice displayed slower development with apparent lower body mass than wt, while Tg10 littermates were smaller than those from Tg37 (Fig. 3A). The other signs of developmental defects were reduced cage activity of Tg mice compared to wt mice owing to restricted capacity of splaying lower limbs of Tg mice (Fig. 3B). The observation of defective hind limb activity may be attributed to muscle weakness. To determine whether the muscle weakness in

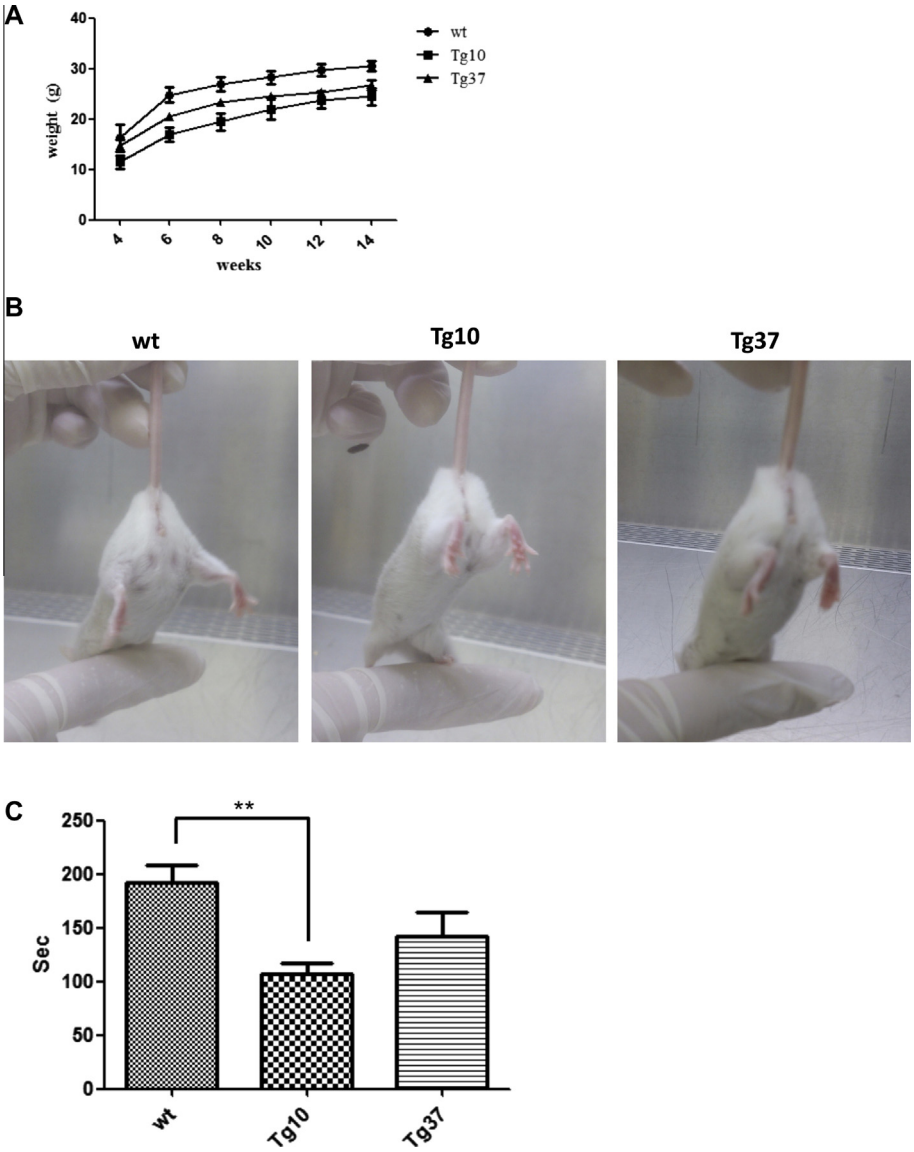

Fig. 3. Pnn CCD transgene expression correlates with impaired skeletal muscle function in transgenic mice. (A) Comparative body mass of wt versus Tg mice from 4 to 12 weeks of age. (B) Pnn mutant mice develop restricted capacity to splay lower limbs. (C) Motor dysfunction of Pnn mutant mice. The Rotarod accelerating test was performed on wt ($n = 7$), Tg10 ($n = 4$) and Tg37 ($n = 3$) mice at 3 months of age. Error bars represent the SEM of three independent experiments. One-way Anova test. $^{**}P < 0.01$.

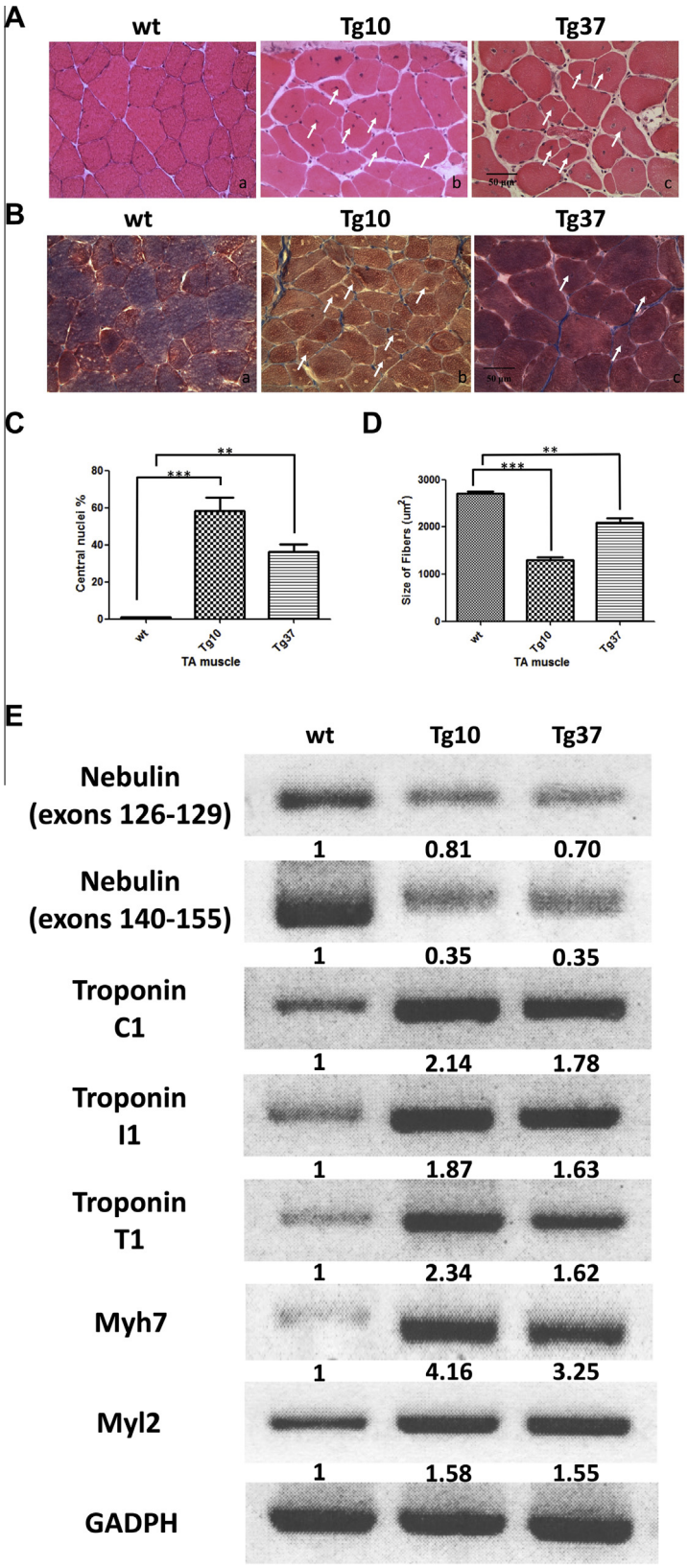

Fig. 4. Skeletal muscles from Pnn mutant mice show dystrophic histologic features and aberrant expression of NEB and slow type fiber genes. HE (A) and Masson-trichome (B) stained cryo-cross sections of TA muscle from wild-type (a), Tg10 (b) and Tg37 (c) Tg mice at 3 months of age. Arrows indicate central nuclei. Note the increased connective tissue (blue color) surrounding muscle fibers in Tg mice compared to the wt control. (C) Increased central nucleus numbers in TA muscle from Tg10 ($n = 3$) and Tg37 ($n = 3$) mice versus those from wt ($n = 3$) control at 3 months of age. Calculation of 300 muscle fibers per mice. (D) Histogram of cross-sectional muscle fiber area shows muscle fiber atrophy in TA muscles from Tg 10 and Tg 37 mice. Calculation of 300 muscle fibers per mice. Error bars represent the SEM of three independent experiments. One-way Anova test. $^{**}P < 0.01$, $^{***}P < 0.001$. (E) Semi-quantitative RT-PCR of selective genes differentially expressed in the gene expression microarray. Numbers below each lane represent fold increase/decrease relative to the wt control. (For interpretation of the references to color in this figure legend, the reader is referred to the web version of this article.)

Table 1
Top 10 enrichment pathway terms from gene set enrichment analysis (Base on k/K value).

Geneset name	Gene overlap (k)	Count	Gene set (K)	Description	k/K
Striated muscle contraction	MYL2, TNNC1, MYH8, TNNI1, NEB, TNNT1	6	27	Genes involved in striated muscle contraction	0.222
Platelet calcium homeostasis	ATP2A2, STIM, SLC8A2, ATP2B3	4	18	Genes involved in platelet calcium homeostasis	0.222
IL23 pathway	SOCS3, TYK2, NFKB1, IL17F	4	37	IL23-mediated signaling events	0.108
IL6 pathway	SOCS3, TYK2, IRF1, PIAS1, MAP2K6	5	47	IL6-mediated signaling events	0.106
E-cadherin stabilization pathway	MYL2, ENAH, CYFIP2, EXOC4	4	42	Stabilization and expansion of the E-cadherin adherens junction	0.095
Hypertrophic cardiomyopathy HCM	MYL2, TNNC1, ITGAV, ATP2A2, CACNB1, LMNA, DAG1, PRKAG3	8	85	Hypertrophic cardiomyopathy (HCM)	0.094
HDAC pathway	MAP2K6, MEF2C, NFATC2	3	32	Control of skeletal myogenesis by HDAC and calcium/calmodulin dependent kinase (CaMK)	0.093
Respiratory electron transport	UQCRQ, SDHB, NDUFA8, NDUFA9, NDUFB2, NDUFB5, NDUFA11	7	79	Genes involved in respiratory electron transport	0.088
NFAT pathway	EGR1, NFATC2, MAF, PTPRK	4	47	Calcineurin-regulated NFAT-dependent transcription in lymphocytes	0.085
Deadenylation dependent mRNA decay	LSM3, LSM1, RQCD1, TNKS1BP1	4	48	Genes involved in deadenylation-dependent mRNA decay	0.083

Pnn mutant Tg mice affected muscle function, we performed exercise tolerance tests with Rotarod apparatus on mice at 3 months of age (Fig. 3C). Rotarod performance was markedly impaired in Tg mice compared to wt controls (time to fall at 10 rpm 100 s versus >200 s for wt mice). Collectively, Pnn mutant Tg mice were characterized as having a muscle wasting phenotype during development and apparent muscle weakness as demonstrated by the Rotarod accelerating test.

Skeletal muscles from Pnn mutant Tg mice showed dystrophic histological features characterized by variability of muscle fiber size, internal nuclei (Fig. 4A arrows in b and c) and increased connective tissue (Fig. 4B). Quantification of the number of centrally nucleated fibers, a hallmark of myopathy and muscle regeneration, showed a comparatively high level of central nuclei in Pnn Tg mice relative to the wt controls (Fig. 4C). Notably, different muscle types in Tg mice, either from founder 10 or 37, was affected to various extents and showed diverse numbers of central nuclei (Supplementary Fig. 3A) with TA (58%) and gastrocnemius (GS, 48%) muscles loaded with highest number of central nuclei (Supplementary Fig. 3B). Morphometric analysis of HE stained TA muscles revealed that the first alteration in Pnn mutant mice appears at around 3 weeks of age with a reduction in the myofiber cross-sectional area (CSA), an assessment of fiber size, compared to the wt control. The extent of the reduction in CSA also varied widely in a single type mutant muscle (Fig. 4D) or among different muscle types (data not shown), indicating that a principal determinant of muscle wasting in Pnn mutant Tg mice was fiber atrophy. Collectively, these data demonstrate aberrant muscle development and impaired muscle function as a result of Pnn CDD mutant ovexpression in Tg skeletal muscle.

3.4. Expression profiling of skeletal muscle of Pnn mutant mice

To explore the molecular mechanism underlying the phenotype, we conducted gene expression profiling of TA muscle from Tg 10 and wt mice at 3 months of age ($n = 3$), when dystrophic symptoms were present with pronounced central nucleated fibers, using MOA v.2.1 mouse OneArray (Phalanx Biotech Group, Taiwan). 1559 genes were differentially expressed (upregulated 683; downregulated 876) in Tg and wt samples. Genes differentially expressed with >2 or <−2 log2 value are presented in Supplementary Tables 2 and 3.

To explore whether the differentially expressed genes are represented in gene categories and networks associated with muscular dystrophy, we outputted the gene lists and performed Gene Ontology (GO) biological process analysis and Gene Set Enrichment (GSE) analysis of canonical pathways. The top 10 pathways that the differentially expressed genes belonged to according to GO and GSE analysis are shown in Supplementary Table 4 and Table 1, respectively. Surprisingly, the top pathways from both GO and GSE analysis are associated with striated muscle contraction, which comprise genes involved in regulation of muscle contraction apparatus such as troponin C1, I1, T1, Myl2, Myh8 and NEB (Table 1). With the exception of NEB, which is downregulated, the rest of the genes involved all show elevated expression level. The microarray results were further validated by semiquantitative RT-PCR, which demonstrated a marked reduction in NEB expression (with two primer sets) and a pronounced increase in expression of Myl2, Myh7, Troponins C1, I1 and T1 (Fig. 4E). Notably, all the genes shown to have elevated expression levels by microarray and RT-PCR are of the slow muscle type (type I fiber), indicating that Pnn mutant muscles are susceptible to slow fiber type gene transition in response to debilitating injury.

4. Discussion

Pnn is a SR-related protein without the general RNA recognition motif found in genuine SR protein family members. Interestingly, in lower species like Drosophila, Pnn naturally contains only the CCD domain without the SR domain-enriched C-terminal region generally found in higher species. In this report, we presented data that identify the functional role of the Pnn CCD domain in mouse skeletal muscle development. Tg mice expressing Pnn CCD mutant had reduced body weight, restricted hind limb splay and impaired muscle function (Fig. 3). Skeletal muscles from Pnn Tg mutant mice showed histological features characteristic of muscular dystrophy (Fig. 4). Microarray gene profiling revealed that the deferentially expressed genes belonged to gene categories and networks that are associated with muscular dystrophy. The top category identified (Table 1) includes a number of genes involved in skeletal muscle contraction, particularly those related to muscle contraction in slow-type muscle fibers, such as Myl2, Tnnc1, Tnni1, Tnnt1, Myh7 (Fig. 4E).

It appears that downregulation of expression of endogenous Pnn in Pnn mutant Tg skeletal muscle has a critical role in modulating muscle-specific gene expression because loss of Pnn expression has been reported to be involved in either pre-mRNA splicing or mRNA alternative splicing in cultured cell lines or a gene

targeted mouse model [12,15]. However, depleting Pnn by RNAi or gene targeting approaches resulted in disruption of nuclear speckle structure with a plethora of splicing factors dissembled from speckles [12], which was not observed in the present study in which loss of Pnn expression was through Pnn CDD mutant overexpression (Supplementary Fig. 1). Nevertheless it is clear that aberrant expression of muscle-specific genes in Tg muscles expressing Pnn mutant is associated with reduced endogenous Pnn expression, thereby impairing the mRNA splicing machinery in Tg skeletal muscle.

GSE analysis of canonical pathways indicate that pathophysiological changes associated with Pnn mutant expression may involve striated muscle contraction mechanisms. Among the proteins associated with this mechanism is NEB, an actin-associated protein important for maintenance of sarcomere structure. NEB is downregulated (−1.96-fold) upon microarray profiling and RT-PCR in Pnn Tg skeletal muscle (Fig. 4E). NEB is a giant protein, containing diverse isoforms in the skeletal muscle [16]. Human mutant NEB gene may cause nemaline myopathy (NM) by loss of part of the C-terminal region [17] and deletion of exon 55 [18] leads to severe and intermediate form of NM. In the NEB knockout mice, loss of NEB expression impacts thin filament length, contractility, body mass and appearance of rod-like nemaline bodies [19]. Interestingly, transcriptome-wide array data obtained from skeletal muscles of heterozygous NEB knock-out mice ($NEB^{+/-}$) clearly show five- to eightfold upregulation of slow type troponin (Tn) complex (C1, I1 and T1) and Myh7 [20], a result which correlates with our expression profiling of Pnn mutant skeletal muscles (Fig. 4E). In addition, according to the gene expression profiles, a number of genes are commonly regulated in skeletal muscles of Pnn mutant and $NEB^{+/-}$ mice (Supplementary Table 5). Furthermore in addition to NEB deficiency in skeletal muscles, Pnn mutant mice also share other common features with $NEB^{+/-}$ mice such as reduced contractility force, slow body growth, fiber size variation and transition of muscle type gene from fast to slow. It is, therefore, conceivable that reduced Pnn expression may downregulate NEB expression through differential pre-mRNA/alternative splicing of NEB leading to functional inactivation of this protein in a process similar to that occurs in NM disease. In the future, it will be interesting to examine NM disease-associated defects in Pnn mutant skeletal muscle to further correlate the relationship between loss of Pnn expression and NM disease.

In conclusion, Pnn mutant expression induces aberrant skeletal muscle development leading to a muscular dystrophy-like phenotype in Tg mice. These data imply that although the Pnn CCD domain occurs naturally in Drosophilia and is conserved across all species examined (Fig. 1A), it is incapable of replacing the full length Pnn normally found in vertebrates, which still require full length Pnn for functions that rely on the N-terminal CCD domain and RS domains located in the C-terminal region. The Tg mouse generated by overexpression of the Pnn CCD domain displays many characteristics resembling $NEB^{+/-}$ mice and may therefore represent an animal model of skeletal muscle pathology with NEB deficiency.

Acknowledgments

This research was supported by Grants from Chang Gung Memorial Hospital (CMRPD1B0431), the Ministry of Education (Tope Center Grant, EMRPD 1C0151) and the National Science Council (NSC-101-2320-B-182-003-MY3), ROC.

Appendix A. Supplementary data

Supplementary data associated with this article can be found, in the online version, at http://dx.doi.org/10.1016/j.bbrc.2013.11.108.

References

[1] P. Ouyang, S.P. Sugrue, Identification of an epithelial protein related to the desmosome and intermediate filament network, J. Cell Biol. 118 (1992) 1477–1488.
[2] P. Ouyang, S.P. Sugrue, Characterization of pinin, a novel protein associated with the desmosome-intermediate filament complex, J. Cell Biol. 135 (1996) 1027–1042.
[3] J.M. Brandner, S. Reidenbach, C. Kuhn, W.W. Franke, Identification and characterization of a novel kind of nuclear protein occurring free in the nucleoplasm and in ribonucleoprotein structures of the "speckle" type, Eur. J. Cell Biol. 75 (1998) 295–308.
[4] N. Saitoh, C.S. Spahr, S.D. Patterson, P. Bubulya, A.F. Neuwald, D.L. Spector, Proteomic analysis of interchromatin granule clusters, Mol. Biol. Cell 15 (2004) 3876–3890.
[5] G. Zimowska, Pinin/DRS/memA interacts with SRp75, SRm300 and SRrp130 in corneal epithelial cells, Invest. Ophthalmol. Vis. Sci. 44 (2003) 4715–4723.
[6] C. Li, R.I. Lin, M.C. Lai, P. Ouyang, W.Y. Tarn, Nuclear Pnn/DRS protein binds to spliced mRNPs and participates in mRNA processing and export via interaction with RNPS1, Mol. Cell. Biol. 23 (2003) 7363–7376.
[7] M.S. Jurica, L.J. Licklider, S.R. Gygi, N. Grigorieff, M.J. Moore, Purification and characterization of native spliceosomes suitable for three-dimensional structural analysis, RNA 8 (2002) 426–439.
[8] T.O. Tange, T. Shibuya, M.S. Jurica, M.J. Moore, Biochemical analysis of the EJC reveals two new factors and a stable tetrameric protein core, RNA 11 (2005) 1869–1883.
[9] Q. Pan, O. Shai, L.J. Lee, B.J. Frey, B.J. Blencowe, Deep surveying of alternative splicing complexity in the human transcriptome by high-throughput sequencing, Nat. Genet. 40 (2008) 1413–1415.
[10] T.A. Cooper, C.P. Ordahl, A single cardiac troponin T gene generates embryonic and adult isoforms via developmentally regulated alternate splicing, J. Biol. Chem. 260 (1985) 11140–11148.
[11] C.D. Chen, R. Kobayashi, D.M. Helfman, Binding of hnRNP H to an exonic splicing silencer is involved in the regulation of alternative splicing of the rat beta-tropomyosin gene, Genes Dev. 13 (1999) 593–606.
[12] S. Leu, Y.M. Lin, C.H. Wu, P. Ouyang, Loss of Pnn expression results in mouse early embryonic lethality and cellular apoptosis through SRSF1-mediated alternative expression of Bcl-xS and ICAD, J. Cell Sci. 125 (2012) 3164–3172.
[13] J.H. Joo, Y.J. Lee, G.C. Munguba, Role of Pinin in neural crest, dorsal dermis, and axial skeleton development and its involvement in the regulation of Tcf/Lef activity in mice, Dev. Dyn. 236 (2007) 2147–2158.
[14] S.Y. Hsu, Y.C. Cheng, H.Y. Shih, P. Ouyang, Dissection of the role of Pinin in the development of zebrafish posterior pharyngeal cartilages, Histochem. Cell Biol. 138 (2012) 127–140.
[15] J.H. Joo, G.P. Correia, J.L. Li, M.C. Lopez, H.V. Baker, S.P. Sugrue, Transcriptomic analysis of PNN- and ESRP1-regulated alternative pre-mRNA splicing in human corneal epithelial cells, Invest. Ophthalmol. Vis. Sci. 54 (2013) 697–707.
[16] K. Donner, M. Sandbacka, V.L. Lehtokari, C. Wallgren-Pettersson, K. Pelin, Complete genomic structure of the human nebulin gene and identification of alternatively spliced transcripts, Eur. J. Hum. Genet. 12 (2004) 744–751.
[17] C. Wallgrenttersson, K. Donner, C. Sewry, Mutations in the nebulin gene can cause severe congenital nemaline myopathy, Neuromuscul. Disord. 12 (2002) 674–679.
[18] V.L. Lehtokari, R.S. Greenleaf, E.T. DeChene, The exon 55 deletion in the nebulin gene – one single founder mutation with world-wide occurrence, Neuromuscul. Disord. 19 (2009) 179–181.
[19] C.C. Witt, C. Burkart, D. Labeit, Nebulin regulates thin filament length, contractility, and Z-disk structure in vivo, EMBO J. 25 (2006) 3843–3855.
[20] C. Gineste, J.M. De Winter, C. Kohl, In vivo and in vitro investigations of heterozygous nebulin knock-out mice disclose a mild skeletal muscle phenotype, Neuromuscul. Disord. 23 (2013) 357–369.